Local Field Asymmetry Drives Second-Harmonic Generation in Noncentrosymmetric Nanodimers

ARTICLE *in* NANO LETTERS · MAY 2007

Impact Factor: 13.59 · DOI: 10.1021/nl0701253 · Source: PubMed

NANO LETTERS

2007
Vol. 7, No. 5
1251−1255

Local Field Asymmetry Drives Second-Harmonic Generation in Noncentrosymmetric Nanodimers

Brian K. Canfield,* Hannu Husu, Janne Laukkanen,† Benfeng Bai,† Markku Kuittinen,† Jari Turunen,† and Martti Kauranen

Institute of Physics, Optics Laboratory, Tampere University of Technology, P.O. Box 692, FI-33101 Tampere, Finland

Received January 17, 2007; Revised Manuscript Received March 16, 2007

ABSTRACT

We demonstrate that second-harmonic generation (SHG) from arrays of noncentrosymmetric T-shaped gold nanodimers with a nanogap arises from asymmetry in the local fundamental field distribution and is not related strictly to nanogap size. Calculations show that the local field contains orthogonal polarization components not present in the exciting field, which yield the dominant SHG response. The strongest SHG responses occur through the local surface susceptibility of the particles for a fundamental field distributed asymmetrically at the particle perimeters. Weak responses result from more symmetric distributions despite high field enhancement in the nanogap. Nearly constant field enhancement persists for relatively large nanogap sizes.

A great deal of the recent interest in the optical responses of metal nanoparticles, nanoapertures in metal films, and metamaterials focuses on enhancing local electromagnetic fields to facilitate light−matter interactions. Random and fractal metal clusters have been predicted to lead to giant enhancements of the local electric field.[1−3] Strong local fields are particularly important for nonlinear optical processes, such as surface-enhanced Raman scattering and second-harmonic generation (SHG),[4−7] which scale with a high power of the field.[8] Indeed, field enhancement by rough metal surfaces has enabled the sensing of single molecules by surface-enhanced Raman scattering.[9] Controllable local-field enhancement would also benefit other photonics applications such as nanoscale antennae that operate at optical wavelengths,[10,11] nanoscale lenses for subwavelength focusing and photolithography,[12] two-photon microscopy,[13] and even magnetically resonant metamaterials.[14,15]

Enormous enhancement factors of 10^3-10^6 compared to the fundamental electric field at a flat metal surface have been calculated for closely spaced "designer" metal nanostructures such as chains of self-similar metal spheres, disks, and truncated tetrahedral prisms.[16−18] These large values were predicted for gaps of just a few nm ("nanogaps") between nanoparticles. However, very small features such as particle separations of less than 10 nm are exceptionally difficult to fabricate lithographically,[19] and particle boundaries are often less than ideal.[20] Actual nanogaps thus tend to be both substantially larger and less well-defined than their theoretical counterparts. As a consequence, experimentally obtained enhancement factors are often far less impressive, generally only 1−2 orders of magnitude.[21−23]

Symmetry of the nanostructure and polarization of the field also play very important roles in field enhancement. For nanodimer systems formed by stripes,[11] tip-to-tip triangle "bowties",[24] intersecting cylinders[19,25] and even cylindrical apertures in a metal film,[26] high enhancement is observed only when the incident polarization is aligned parallel to the interparticle axis. Illuminating the sample with the perpendicular polarization yields significantly less enhancement. The special role of this axial direction has also been emphasized in the less symmetric case of enhanced SHG from the tip of a near-field optical microscope.[27]

In most cases, the effects exhibiting the highest enhancements have depended mainly on the intensity of the local field. However, additional phase and symmetry considerations dictate that second-order nonlinear optical processes (such as SHG) require noncentrosymmetry.[8] Therefore, strong fields alone may not be sufficient for SHG if the sample is centrosymmetric. Several of the two-dimensional lithographic designer structures on a substrate appear centrosymmetric when investigated at normal incidence,[11,19,25,26] although structures with lower in-plane symmetry have also been presented.[16,28,29] A chain of self-similar spheres, on the other hand, forms a noncentrosymmetric system and is predicted to enhance SHG by a (nonresonant) factor of $\sim 10^4$, but only for very small sphere separations of a few nm.[30]

We provide here experimental evidence supported by numerical calculations that the intensity of SHG from arrays

* Corresponding author. E-mail: brian.canfield@tut.fi.
† Department of Physics and Mathematics, University of Joensuu, P.O. Box 111, FI-80101 Joensuu, Finland.

10.1021/nl0701253 CCC: $37.00
Published on Web 03/31/2007

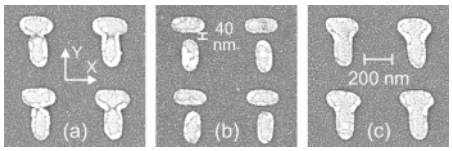

Figure 1. SEM images of T-shaped gold nanoparticles. (a) noncontacted 0 nm nanogap, (b) 40 nm nanogap, (c) fully contacted. The scale in (c) is the same for all three SEMs.

of noncentrosymmetric T-shaped gold nanodimers with a nanogap does not depend strictly on the nanogap size and having a strong local field in the nanogap. Instead, asymmetry in the distribution of the induced local field at the fundamental wavelength and its interaction through the local surface susceptibility of the nanodimers play key roles. We applied rigorous diffraction theory to calculate the local field distributions as a function of nanogap size. The induced local field exhibits orthogonal polarization components, not present in the incident exciting field, that yield the dominant SHG response. The calculations also reveal that the symmetry of the field distribution varies with nanogap size in a more complicated manner than simple size dependence. As opposed to more symmetric nanodimer systems, field enhancement occurs for both incident field polarizations and, counter intuitively, persists up to relatively large nanogap sizes of several tens of nm.

We fabricated several square arrays (0.9 mm per side) of T-shaped gold nanoparticles on the same fused silica substrate using electron beam lithography.[29] The "T" is formed by properly orienting separate horizontal and vertical bars. We introduced nanogaps between the bars ranging from a "barely contacted" 0 nm shown in the scanning electron micrograph (SEM) image in Figure 1a to a well-separated 40 nm in Figure 1b. For comparison, we also fabricated an array of fully contacted T's, as shown in Figure 1c. The structural design of the T's suggests a natural X−Y coordinate system as depicted in Figure 1a; consequently, a single mirror-symmetry axis lies along Y. While an ideal T structure would be formed by rectangular bars with square corners, the actual bars exhibit rounded corners (a "stadium" shape). All bars were intended to be of equal length (approximately 250 nm), although difficulties in the fabrication process (such as beam astigmatism) caused variations of up to 10% in this value, most commonly in the horizontal bars. The line width of all bars is 125 nm, the gold thickness is 20 nm, and the grating spacing in all arrays is 500 nm. The arrays are also protected by a 20 nm thick layer of fused silica.

Prior to SHG measurements, we measured the extinction spectra of the arrays for both X- and Y-polarizations using fiber optic spectrometers and a white light source (Supporting Information). The main extinction resonances in metal nanoparticles arise from collective dipolar oscillations of conduction electrons (usually denoted "plasmons"), and the peak wavelength depends on the plasmon oscillation length (i.e., bar length).[25,31,32] Although some of the bars in the 0 nm array of Figure 1a visually appear to be contacted, the Y-polarized extinction spectra in Figure 2 clearly indicate that the bars of this array respond separately and distinctly,

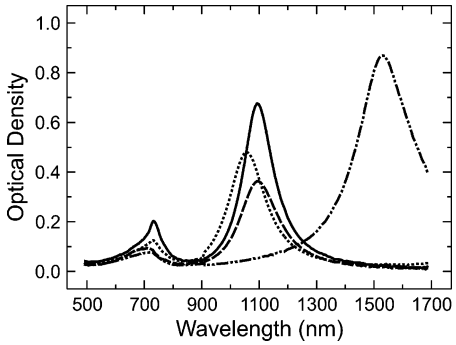

Figure 2. Y-polarized extinction spectra for different nanogap sizes. Dots: 0 nm nanogap; solid line: 15 nm nanogap; dashes: 40 nm nanogap. For comparison, the spectrum of fully contacted T's is included (dash−dots).

like those of the larger-nanogap arrays. The isolated vertical bars from larger-nanogap arrays (being all about the same length) display resonance peaks near 1100 nm, with the 0 nm nanogap (where the vertical bars are slightly shorter) nearby at 1060 nm. The much longer oscillation path length in the fully contacted array of Figure 1c, on the other hand, results in a resonance peak location at a much longer wavelength of 1530 nm. The X-polarization resonances exhibit more variation in the peak location (1100 ± 100 nm) because of differences in bar length resulting from the fabrication process as described earlier. The smaller resonances below 750 nm are due to the (transverse) linewidths of the horizontal bars,[31] but as they lie far from both the fundamental laser wavelength at 1060 nm and the second-harmonic wavelength at 530 nm, we neglect them.

The SHG responses of the arrays were measured using a simple one-beam, normal-incidence geometry (Supporting Information, Figure S1). Because of normal incidence, the polarizations of the fundamental and SHG fields can be expressed in the same X−Y coordinate system as the sample, and electric-dipole-type selection rules apply.[31] The mirror symmetry with respect to the Y axis dictates that the allowed signals are YYY, YXX, XYX, and XXY, where the two last indices refer to the polarization of the fundamental beam (which acts twice) and the first to that of the SHG beam. Of these, we measure the YYY and YXX signals, which represent the pure polarization combinations of the output SHG and input fundamental fields.

The intensities of the SHG responses YXX (circles) and YYY (triangles) are shown in Figure 3 as a function of nanogap size, normalized by setting the weakest response to unity. The SHG responses clearly depend on the size of the nanogap, but not in smoothly decreasing functions as might be inferred from theory.[30] The largest nanogap (40 nm) yields weak SHG responses for both components, as might be expected from theory that predicts that the nanogap must be small (a few nm or less) to enhance the SHG response[25,30] and from experimental evidence of overlapping cylindrical apertures.[26] Another consideration applies as well: as the nanogap size increases, the whole structure approaches a centrosymmetric configuration of alternating horizontally and vertically oriented bars, which would inhibit an SHG response.[8] The largest SHG response in Figure 3

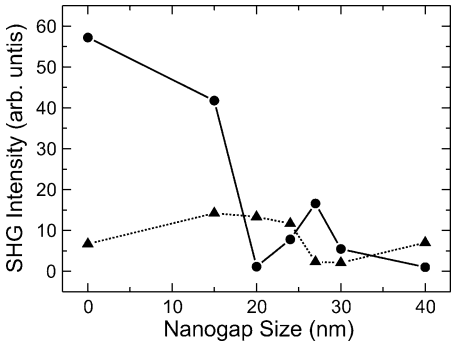

Figure 3. SHG responses. Circles: YXX; triangles: YYY. The intensities have been normalized so that the smallest response equals 1. The solid and dotted lines are visual guides.

occurs for YXX from the 0 nm nanogap and is about a factor of 50 larger than the response from the 40 nm nanogap array. This result is also in accordance with theoretical calculations,[25,30] although the enhancement observed here is smaller.

However, the most striking features of Figure 3 cannot be readily explained merely by requiring a small nanogap. Although both X- and Y-polarizations are approximately equally resonant at the fundamental, the YYY response is much weaker than the YXX response for smaller nanogaps. The YYY response grows with increasing nanogap size up to 20 nm, as opposed to the decreasing YXX response. Also, the origin of the drop and recovery of the YXX response in the 20−30 nm nanogap range is mysterious. To explain these issues, it is necessary to consider both the symmetry of a T-particle and the local fundamental electric field distribution in an array unit cell.

Local electric field distributions at 1060 nm (fundamental wavelength) and 530 nm (wavelength of second-harmonic) were calculated in a unit cell using the Fourier modal method[33] for both X− and Y-polarized incident fields of unit magnitude (Supporting Information). The calculations reveal that the fundamental X-polarized field component localizes at the ends of the horizontal bar, while the Y-component concentrates in the nanogap region (cf., Figure 4). However, at 530 nm, no strong local fields are observed (enhancement factors are less than 1.7 for X-polarization and 1.3 for Y-polarization), the distributions remain unaffected by the presence of the nanogap, and the field never localizes in the nanogap. Therefore, the SHG response is indeed driven by localized enhancement of the nearly resonant fundamental field. Moreover, this result agrees with previous findings that SHG from nanostructured metal surfaces results from overlapping eigenmodes of the fundamental and second-harmonic fields,[34] especially from where the local configuration is asymmetric.[7] However, in our case, the local field effects at the SHG wavelength are weak, and the response is therefore dominated by the strong and asymmetric local fundamental fields.

The strongest fundamental fields occur close to the particle boundaries, meaning that the SHG responses arise through the local surface susceptibility of the metal particles. The total SHG response thus results from integration of the local response along the particle perimeters (Supporting Information). The structure of the local tensor implies that contributions from the portions of the perimeters possessing opposite surface normals tend to cancel.[8] Therefore, the more symmetrically the local field is distributed along the perimeters, the weaker we expect the SHG response to be. Moreover, although the nanogap region itself is formally noncentrosymmetric, the responses from the horizontal bar bottom and the vertical bar endcap have a strong tendency to cancel when the local field is evenly distributed across the nanogap (Supporting Information, Figure S2).

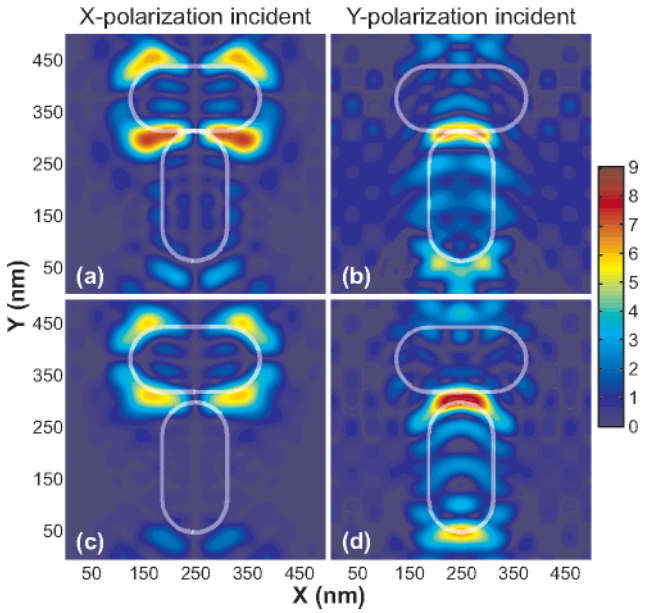

Figure 4. Electric field Y-component distributions for incident X- and Y-polarizations, as indicated by the column headings: (a,b) 1 nm nanogap; (c, d) 20 nm nanogap.

The polarization behavior of the field displays intriguing behavior that, while not readily apparent from the SHG experiment, nevertheless agrees well and helps explain the unanticipated results. We note that the induced local fundamental field contains orthogonal polarization components not present in the exciting field. For instance, a purely X-polarized incident field induces a local Y-component comparable in magnitude to the local X-component, as depicted in Figure 4a and c for 1 and 20 nm nanogaps. For the dimer with 1 nm nanogap, this Y component localizes around the horizontal bar but is distributed asymmetrically, with strong enhancement around the nanogap region and the bar surface. This induced polarization component, coupled with its asymmetric distribution, comprises the origin of the dominant SHG response, YXX, in good agreement with the high response of the 0 nm nanogap in Figure 3. The sample with a 20 nm nanogap, on the other hand, shows not only much weaker enhancement but a more symmetrical distribution, which then explains the low YXX response at 20 nm in Figure 3. The calculations also show that the asymmetric distribution of Figure 4a partially recovers for even larger (25−35 nm) gap sizes, which explains the secondary YXX peak in the experimental data.

With the nanogap positioned at the end of the vertical bar, one might expect the field to localize in the nanogap region

better for incident Y-polarization from simple electromagnetic considerations. Surprisingly, we find that the strongest fields in Figure 4b lie not in the nanogap itself but slightly off to the sides. In fact, the highest field concentrations for the smallest nanogaps (≤15 nm) do not localize strictly within the narrowest nanogap region for either polarization, nor do they necessarily occur at the metal surface. Our T design thus leads to an entirely different situation than the case of self-similar spheres, where the field was predicted to localize directly between the spheres in a nanogap of ∼5 nm.[16,30]

In addition, the strong field is evenly distributed between the horizontal bar bottom and the vertical bar endcap, leading to suppression of the SHG response.[30] For our T's, the nanogap must be substantially larger (20 nm) before the Y-component finally localizes within the nanogap, as seen in Figure 4d. Close inspection reveals that the peak field is now located closer to vertical bar endcap, yielding the growth in the SHG response shown in Figure 3 for incident Y-polarization over the 15−25 nm nanogap range. However, despite high enhancement, the Y-component distribution for incident Y-polarization is more symmetric in all cases, resulting in the overall weaker YYY responses in Figure 3.

For both incident polarizations, the local fundamental field is enhanced by roughly a factor of 8. Enhancement for X-polarized input remains relatively constant for the smaller and larger nanogap ranges, but drops in the middle range of 20−30 nm (Supporting Information, Figure S3). This slight decrease alone is not enough to explain the very low YXX response at 20 nm in Figure 3, though. The symmetrical field distribution shown in Figure 4c must be considered as well. Y-polarization, on the other hand, increases very slightly up to 35 nm and decays beyond that point. Thus, strong fundamental field enhancement persists even for relatively large nanogaps. Also, the highest SHG response occurs for YXX although both X− and Y-polarizations exhibit nearly the same enhancement factor, countering the argument that enhancement due to small nanogap size only is sufficient to increase the SHG response.

In summary, we have observed that SHG from T-shaped gold nanodimers with nanogaps depends more strongly on polarization and the symmetry of the local fundamental field distribution than on the nanogap size. It is evident that asymmetrical nanoparticle designs and field polarization considerations merit further study, as they may offer exciting new opportunities for photonic applications of metal nanoparticles. The asymmetry argument runs counter to the conventional findings of more symmetric systems that only one fundamental polarization induces enhancement and that a small nanogap alone is sufficient to enhance the SHG response. These results also demonstrate that full understanding of the nonlinear optical properties of nanostructures requires consideration of not only the local field distribution but also its polarization properties. Furthermore, potentially large field enhancements may be obtained even for relatively large nanogap sizes, which could relax the necessity of exceptionally small features that are difficult to fabricate. Finally, the results suggest that approaches seeking to describe the nonlinear response in terms of average quantities or effective media may be inappropriate.

Acknowledgment. This work was supported by grant 102018 from the Academy of Finland.

Supporting Information Available: Additional discussion of experimental procedures (Figure S1), local field distribution calculation details, a simple example of how symmetric local field distribution couples to the local surface susceptibility in the nanogap region and weakens the SHG response (Figure S2), local field enhancement factors as a function of nanogap size (Figure S3), and supporting references. This material is available free of charge via the Internet at http://pubs.acs.org.

References

(1) Markel, V. A.; Shalaev, V. M.; Stechel, E. B.; Kim, W.; Armstrong, R. L. *Phys. Rev. B* **1996**, *53*, 2425−2436.
(2) Sarychev, A. K.; Shubin, V. A.; Shalaev, V. M. *Phys. Rev. B* **1999**, *60*, 16389−16408.
(3) Karpov, S. V.; Gerasimov, V. S.; Isaev, I. L.; Markel, V. A. *Phys. Rev. B* **2005**, *72*, 205425.
(4) Agarwal, G. S.; Jha, S. S. *Solid State Commun.* **1982**, *41*, 499−501.
(5) Chen, C. K.; Heinz, T. F.; Ricard, D.; Shen, Y. R. *Phys. Rev. B* **1983**, *27*, 1965−1979.
(6) Shalaev, V. M.; Poliakov, E. Y.; Markel, V. A. *Phys. Rev. B* **1996**, *53*, 2437−2449.
(7) Stockman, M. I.; Bergman, D. J.; Anceau, C.; Brasselet, S.; Zyss, J. *Phys. Rev. Lett.* **2004**, *92*, 057402.
(8) Boyd, R. W. *Nonlinear Optics*; Academic Press: San Diego, 1992.
(9) Kneipp, K.; Wang, Y.; Kneipp, H.; Perelman, L. T.; Itzkan, I.; Dasari, R. R.; Feld, M. S. *Phys. Rev. Lett.* **1997**, *78*, 1667−1670.
(10) Fromm, D. P.; Sundaramurthy, A.; Schuck, P. J.; Kino, G.; Moerner, W. E. *Nano Lett.* **2004**, *4*, 957−961.
(11) Mühlschlegel, P.; Eisler, H.-J.; Martin, O. J. F.; Hecht, B.; Pohl, D. W. *Science* **2005**, *308*, 1607−1609.
(12) Sundaramurthy, A.; Schuck, P. J.; Conley, N. R.; Fromm, D. P.; Kino, G. S.; Moerner, W. E. *Nano Lett.* **2006**, *6*, 355−360.
(13) Anceau, C.; Brasselet, S.; Zyss, J.; Gadenne, P. *Opt. Lett.* **2003**, *28*, 713−715.
(14) Pakizeh, T.; Abrishamian, M. S.; Granpayeh, N.; Dmitriev, A.; Käll, M. *Opt. Express* **2006**, *14*, 8240−8246.
(15) Klein, M. W.; Enkrich, C.; Wegener, M.; Linden, S. *Science* **2006**, *313*, 502−504.
(16) Li, K.; Stockman, M. I.; Bergman, D. J. *Phys. Rev. Lett.* **2003**, *91*, 227402.
(17) Genov, D. A.; Sarychev, A. K.; Shalaev, V. M.; Wei, A. *Nano Lett.* **2004**, *4*, 153−158.
(18) Zou, S.; Schatz, G. C. *Chem. Phys. Lett.* **2005**, *403*, 62−67.
(19) Atay, T.; Song, J.-H.; Nurmikko, A. V. *Nano Lett.* **2004**, *4*, 1627−1631.
(20) Canfield, B. K.; Kujala, S.; Laiho, K.; Jefimovs, K.; Turunen, J.; Kauranen, M. *Opt. Express* **2006**, *14*, 950−955.
(21) Aizpurua, J.; Hanarp, P.; Sutherland, D. S.; Käll, M.; Bryant, G. W.; de Abajo, F. J. G. *Phys. Rev. Lett.* **2003**, *90*, 057401.
(22) Abe, S.; Kajikawa, K. *Phys. Rev. B* **2006**, *74*, 035416.
(23) Schuck, P. J.; Fromm, D. P.; Sundaramurthy, A.; Kino, G. S.; Moerner, W. E. *Phys. Rev. Lett.* **2005**, *94*, 017402.
(24) Sundaramurthy, A.; Crozier, K. B.; Kino, G. S.; Fromm, D. P.; Schuck, P. J.; Moerner, W. E. *Phys. Rev. B* **2005**, *72*, 165409.
(25) Romero, I.; Aizpurua, J.; Bryant, G. W.; de Abajo, F. J. G. *Opt. Express* **2006**, *14*, 9988−9999.
(26) Lesuffleur, A.; Kumar, L. K. S.; Gordon, R. *Appl. Phys. Lett.* **2006**, *88*, 261104.
(27) Bouhelier, A.; Beversluis, M.; Hartschuh, A.; Novotny, L. *Phys. Rev. Lett.* **2003**, *90*, 013903.
(28) Lamprecht, B.; Leitner, A.; Aussenegg, F. R. *Appl. Phys. B* **1999**, *68*, 419−423.
(29) Tuovinen, H.; Kauranen, M.; Jefimovs, K.; Vahimaa, P.; Vallius, T.; Turunen, J.; Tkachenko, N. V.; Lemmetyinen, H. *J. Nonlinear Opt. Phys. Mater.* **2002**, *11*, 421−432.

(30) Li, K.; Stockman, M. I.; Bergman, D. J. *Phys. Rev. B* **2005**, *72*, 153401.
(31) Canfield, B. K.; Kujala, S.; Kauranen, M.; Jefimovs, K.; Vallius, T.; Turunen, J. *J. Opt. A: Pure Appl. Opt.* **2005**, *7*, 110−117.
(32) Prescott, S. W.; Mulvaney, P. *J. Appl. Phys.* **2006**, *99*, 123504.
(33) Li, L. *J. Opt. A: Pure Appl. Opt.* **2003**, *5*, 345−355.
(34) Bozhevolnyi, S. I.; Beermann, J.; Coello, V. *Phys. Rev. Lett.* **2003**, *90*, 197403.

NL0701253